

Bistability Experimentally Observed at Three Milliwatts in Indium Arsenide and Theoretically Predicted for a New Class of Nonlinear Dielectrics

E. Garmire, C. D. Poole and J. A. Goldstone

Phil. Trans. R. Soc. Lond. A 1984 **313**, 257-264

doi: 10.1098/rsta.1984.0104

Email alerting service

Receive free email alerts when new articles cite this article - sign up in the box at the top right-hand corner of the article or click [here](#)

To subscribe to *Phil. Trans. R. Soc. Lond. A* go to: <http://rsta.royalsocietypublishing.org/subscriptions>

Bistability experimentally observed at three milliwatts in indium arsenide and theoretically predicted for a new class of nonlinear dielectrics

BY E. GARMIRE, C. D. POOLE AND J. A. GOLDSTONE

Centre for Laser Studies, University of Southern California, Los Angeles, California 90089–1112, U.S.A.

The results of an experimental investigation of nonlinearities and bistability at the band gap in InAs are presented. Bistability was observed in reflection at 3 mW with a HF laser by using the large nonlinearity at the band-gap resonance in InAs. The measured nonlinear refractive index is shown quantitatively to agree with the dynamic Burstein–Moss shift as the mechanism, as long as both the full Fermi–Dirac statistics and the effect of light holes are included in the calculation. In a separate study a theoretical analysis has investigated general conditions for intrinsic bistability without cavities. It is shown that bistability can result from a nonlinear constitutive relation. Specific calculations are presented for bistability due to nonlinear polarization.

This paper is a discussion of recent developments in optical bistability at the University of Southern California, which includes experimental investigations as well as theoretical studies of optical bistability. The results of an experimental investigation of nonlinearities and bistability at the band gap in InAs are presented. Bistability was observed in reflection at 3 mW with a HF laser by using the large nonlinearity at the band gap resonance in InAs. The measured nonlinear refractive index is shown quantitatively to agree with the dynamic Burstein–Moss shift as the mechanism, as long as both the full Fermi–Dirac statistics and the effect of light holes are included in the calculation. In a separate study a theoretical analysis has investigated general conditions for intrinsic bistability without cavities. It is shown that bistability can result from a nonlinear constitutive relation. Specific calculations are presented for bistability due to nonlinear polarization. The experimental discovery of optical bistability in InAs will be discussed first, and the theoretical discussions will be presented in the later parts of the paper.

BISTABILITY IN INDIUM ARSENIDE

Indium arsenide is a III–V semiconductor with a band gap at 3 μm , between the band gap of InSb at 5 μm and GaAs at 1 μm , both of which have previously been shown to exhibit optical bistability near their band gap (Miller *et al.* 1979; Gibbs *et al.* 1979). The reason for investigating InAs is the coincidence of its band gap with the lines of the HF laser, near 3 μm . The results presented here used the 3.096 μm line of the HF laser, which matches the band gap of 2.6×10^{-16} n-type InAs at 77 K. Optical bistability was observed in reflection from a 170 μm thick etalon of InAs, which was polished plane and parallel, and whose back surface was turned into a mirror with silver (Poole & Garmire 1984*a*). The observation of bistability

[67]

in reflection is easier than the observation of bistability in transmission, primarily because of the simplicity of applying 100% reflection to the back face, compared to enhancing the natural 31% Fresnel reflection with multilayer coatings. An additional advantage of studying optical bistability in reflection is the ease with which the sample is heat-sunk. The devices were mounted on a stress-relieving InAs wafer and thence on a copper block. No thermal heating effects from the incident HF laser radiation were observed when this configuration was used. Figure 1 shows experimental results for optical bistability in InAs. In figure 1*a*, switch-on

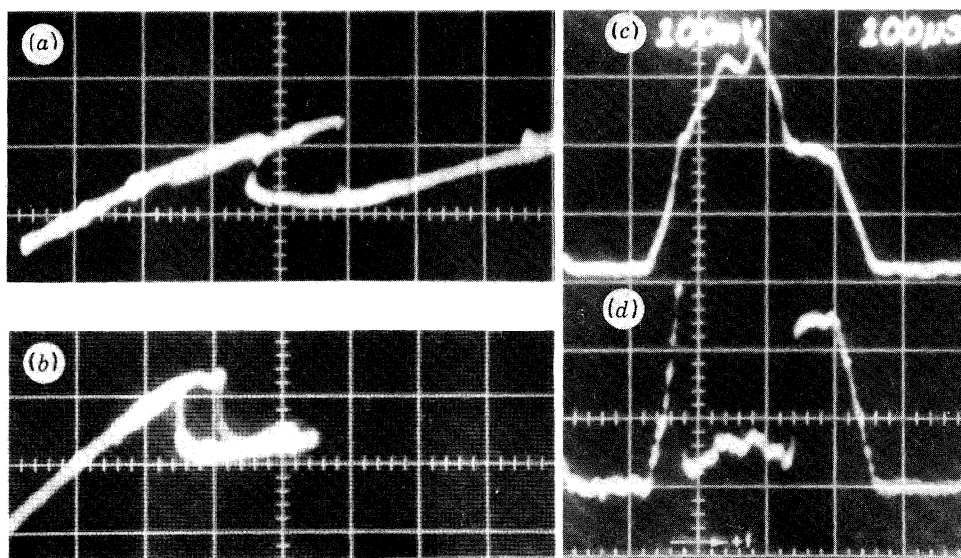


FIGURE 1. Experimental results on whole-beam bistability in InAs. (a), (b) Reflected power against incident power for two different detunings; horizontal scale is 1.5 mW per division, vertical scale is 1 mW per division. (c), (d) Input and reflected signals, respectively, as a function of time.

occurred at 7 mW and is indicated by a drop in the reflected light level. Switch-off occurred at 5 mW and is manifested by a sudden increase in reflectivity of the device. The resulting hysteresis is characteristic of optical bistability. The detuning could be varied by lateral displacement of the etalon, since it was slightly wedge-shaped. The minimum power level at which bistability was observed was 4 mW and is shown in figure 1*b*. The intensity level corresponding to this power level is 75 W cm^{-2} , at the centre of a Gaussian focal spot of width $72 \mu\text{m}$. The hysteresis curves were largest when the output power was monitored at the centre of the beam only. This was achieved by imaging the near field of the etalon onto a $25 \mu\text{m}$ pinhole, placed before the detector. Whole-beam switching is shown here.

The variation in input intensity was obtained by natural pulsations in the HF laser output due to instabilities in its plasma discharge. This led to pulses several hundred microseconds long, as shown in figure 1*c*. The reflected signal as a function of time is shown in figure 1*d*, and the rapid switching of the bistable device to a low-reflecting state is evident. Switching was faster than the time constant of the detector and is expected to be of the order of the lifetime of carriers in InAs, approximately 300 ns.

NONLINEAR REFRACTIVE INDEX IN INDIUM ARSENIDE

The nonlinear index can be inferred from the threshold for bistability and is $3 \times 10^{-5} \text{ cm}^2 \text{ W}^{-1}$. The mechanism that is believed to be responsible for this nonlinear index is the same as that for InSb (Miller *et al.* 1981) and HgCdTe (Hill *et al.* 1982). That is, the dynamic Burstein–Moss shift, or the change in the absorption edge of the band gap due to a filling of the lower levels of the conduction band (Miller *et al.* 1981; Moss 1980). Through the Kramers–Krönig relation, this change in absorption leads to a change in refractive index. Since this change is intensity-dependent, it leads to a nonlinear refractive index.

An accurate experimental determination of the nonlinear refractive index was made by measuring transmission as a function of intensity for an InAs etalon with Fresnel reflection from both surfaces. Fitting these curves to the numerical analysis by using plane wave theory for the transmission of a nonlinear Fabry–Perot etalon with a single value of nonlinear refractive index and linear absorption, for a variety of input phase conditions, allowed a determination of the nonlinear refractive index and the linear absorption. Data for nonlinear transmission curves, their numerical fits and values for n_2 and α inferred from these data are shown in figure 2 for a number of temperatures, which correspond to varying differences of the incident photon

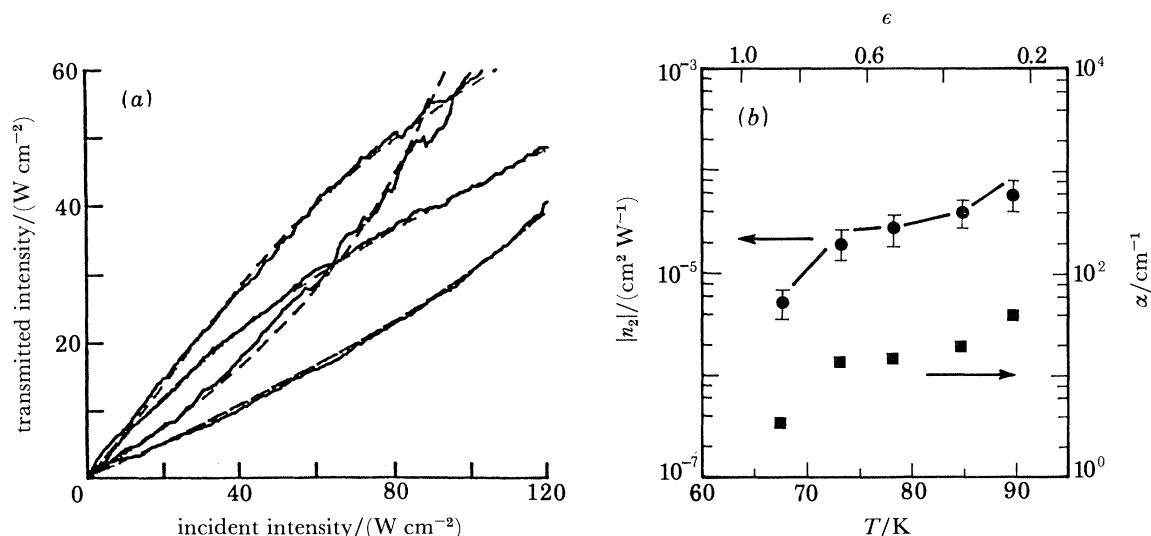


FIGURE 2. Measurements of the nonlinear index in InAs at $3.096 \mu\text{m}$. (a) Nonlinear transmission through an etalon for several detunings and the plane-wave theoretical fit. (b) Summary of results at several temperatures for the nonlinear index n_2 and the linear absorption α . Solid curve is obtained by using (1) with no free parameters. The top scale gives the position of the photon energy relative to the band gap energy ($\epsilon = (E_G - h\nu)/KT$).

energy from the band gap. It is interesting to note that the figure of merit, which is given by n_2/α , is essentially independent of distance from the band gap. This fact will be used later in predicting expected bistability thresholds for other geometries.

To confirm the mechanism for the large nonlinear index, a calculation was made of the nonlinear index at the band gap of direct-band semiconductors. This analysis follows that of Miller *et al.* (1981), but includes the complete Fermi–Dirac statistics required since the semiconductor is degenerate, and also includes the effects of the light-hole band. The absorption

edge is described by the Kane analysis (Kane 1957) and leads to an expression for the figure of merit given by (Poole & Garmire 1984*b*)

$$\frac{n_2}{\alpha} = \frac{-2\pi\tau e^2}{3n_0 k T E_G^3} \left(\frac{\mu_{\text{hh}}}{m_e}\right)^3 P^2 K, \quad (1)$$

where τ is the lifetime of the carriers, P is the momentum element (Kane 1957), μ_{hh} is the mobility of the heavy holes, m_e is the effective mass of the electrons and e is their charge, E_G is the energy of the band gap, n_0 is the linear refractive index, kT is the temperature in energy units, and K is a dimensionless parameter that depends on the carrier concentration and the distance from the band edge, and which has a value close to one. K is shown in figure 3 as

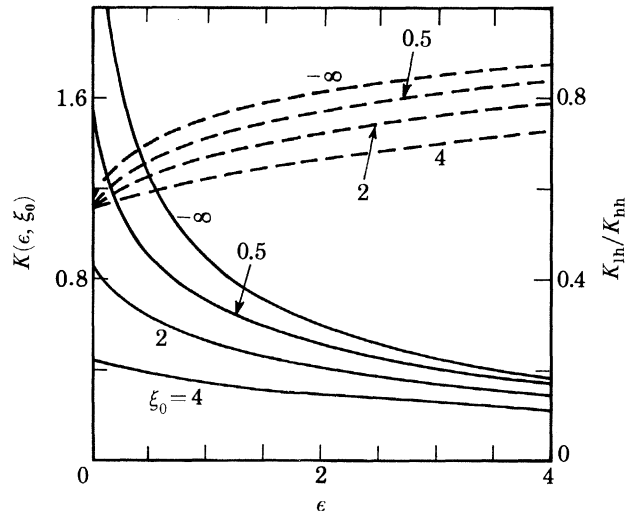


FIGURE 3. $K(\epsilon, \xi_0)$ (solid curves, left scale) and ratio of light-hole contribution to heavy-hole contribution, $K_{\text{lh}}/K_{\text{hh}}$ (broken curves, right scale) against distance from band gap in units of $\epsilon = (E_G - \hbar\omega)/kT$ for several values of the Fermi energy ξ_0 (in units of kT).

a function of distance from the band gap for various values of the Fermi energy. The Fermi energy is related to the carrier concentration in the semiconductor. The larger the Fermi energy, the more impurities in the material. For the impurity levels in the samples used in the experiments reported here, the figure of merit was essentially independent of band gap. This can be seen from figure 2, since in each case $n_2/\alpha = (1.7 \pm 0.3) \times 10^{-6} \text{ cm}^3 \text{ W}^{-1}$. Also included in figure 3 is the ratio of the light hole to the heavy hole contribution, which may reach a value of almost 90%, demonstrating the importance of this term.

To compare experimentally measured nonlinear refractive indices with the theoretical prediction of (1), it is necessary to know the carrier lifetime τ . This was explicitly determined in the sample reported here by monitoring the photoconductivity as a function of time after excitation by a pulse from a Nd:YAG laser; this value was 330 ns.

The excellent agreement between experimental results and theoretical modelling indicates that the dynamic Burstein–Moss shift is indeed the mechanism for the large nonlinear index in InAs at the band gap.

POSSIBILITIES FOR OPTICAL COMPUTATION

From the theory for the nonlinear index, the figure of merit can be used to predict room-temperature operation based on an estimate of the carrier lifetime at room temperature and on the change of band gap with temperature. There is considerable uncertainty in the literature as to the temperature dependence of the lifetime of carriers in InAs. The most optimistic values indicate that liquid phase epitaxial material has a carrier lifetime at room temperature equal to 300 ns (Dalal 1974). This is comparable to the value measured in bulk material at 77 K. The band gap at room temperature corresponds to a wavelength of 3.7 μm . Since the figure of merit is proportional to τ/E_G^3 , the smaller room-temperature band gap and comparable carrier lifetime predict a room-temperature threshold for bistability in l.p.e. InAs even lower than at 77 K in bulk InAs.

Observation of room-temperature bistability requires a laser whose wavelength matches the InAs band gap. The DF laser has lines at 3.7 μm , appropriate to room-temperature operation. This laser is too expensive to operate to provide practical room temperature bistability, however. Another approach would be the HeNe laser at 3.39 μm , which matches the bandgap at 180 K, and operation would be practical using a thermoelectric cooler. Alternatively, the 3.6 μm line in the xenon laser may provide for near-room temperature operation.

To estimate the effectiveness of InAs for optical computations, it is necessary to calculate the minimum power required for switching in an etalon. In the theory for optimization of a nonlinear etalon (Miller 1981), it was found that the critical intensity in the high finesse limit is given by

$$I_c = \lambda\alpha L / (n_2/\alpha), \quad (2)$$

where it is assumed that the loss per pass equals the loss upon reflection; so the thinner the etalon the better. The experiments presented here were for an etalon of 170 μm , optimized according to the calculations of D. A. B. Miller. Under these conditions, the threshold for bistability was 75 W cm^{-2} . An etalon 1.7 μm thick gives a predicted threshold of 0.75 W cm^{-2} . Assuming that the beam can be focused to within a wavelength of light, the minimum predicted threshold power is 100 nW, which gives a capability of 10^6 parallel bits with a 100 mW laser!

In conclusion, the observation of bistability in InAs and comparison with theory suggests the possibility of an extremely impressive room-temperature computational capability.

BISTABILITY DUE TO NONLINEAR CONSTITUTIVE RELATIONS

In addition to experimental studies in InAs, the result of a theoretical study on a new type of optical bistability is outlined. In particular, we wish to point out that optical bistability is possible whenever a medium can be represented by a suitable nonlinear constitutive relation. The constitutive relation is a functional relation between the electric field and some scalar or vector parameters of the system, or both. In the usual formulation of the constitutive relations, material parameters are expressed as functions of the electric field (typically in power series expansions). This formulation necessarily precludes the description of this type of bistability. However, if the electric field is expressed in terms of the material parameters, bistability may be predicted for suitable nonlinear relations. The technique of inverting the expression to obtain the second branch is well known from the theory of bistability in resonant cavities, since the

single-valued expression of the input as a function of the output leads to a multivalued expression for the output as a function of the input.

In our analysis we consider polarization as the material parameter and show that if the electric field is expressed in terms of the polarization, bistability may result. This does not require any explicit feedback, merely the ability to define a constitutive relation. Other examples of this general relation have been presented at this symposium. They include thermal bistability that may result when absorption is the material parameter (M. Dagenais, D. A. B. Miller, C. Klingshirn *et al.*) and bistability that may occur as a result of a change of state within the material, as, for example, in liquid crystals (Y. R. Shen).

BISTABILITY DUE TO NONLINEAR POLARIZATION

To illustrate the general concept we consider here the polarization that results from nonlinear oscillations in molecular or atomic systems. The usual phenomenological description of the polarization as a power series in the electric field obviates the possibility of describing bistability since the electric field is treated as the independent parameter. Thus the second branch cannot be found. A nonlinear model for the general constitutive relation is required before bistability can be postulated. For the purposes of demonstration we use the classical Duffing oscillator as the model of electron oscillation to derive a bistable polarization.

The Duffing oscillator model may be described by the following differential equation for the microscopic material response:

$$m\ddot{x} + \gamma\dot{x} = -Kx - \beta x^2 + eE/m. \quad (3)$$

This is a differential form of the constitutive relation, since the polarization relates to the atomic (or molecular) vibration through $P = Nex$ (for low molecular densities), and the above equation relates x to the electric field. Under these conditions bistability on the microscopic level implies bistability on the macroscopic level. The bistability of the Duffing oscillator is well known and can be calculated by inverting the relation between the amplitude of the oscillation and the force driving the oscillation. For polarization, the driving force is the electric field. We thus look for an expression for the electric field in terms of the amplitude of the oscillation x . Following Duffing, a solution exists at the fundamental frequency given by

$$\{m(\omega_0^2 - \omega^2) - i\gamma\omega + \frac{3}{4}\beta|x|^2\}x = eE. \quad (4)$$

There is an additional relation for the third harmonic, which is here ignored. The cubic form of (4) yields three solutions for the polarization over a range of impressed fields for appropriate parameter choices. Of these three, two are locally stable and one is unstable. Hence a choice of P implies a unique E but the inverse is not true, i.e. $E = E(P)$, but $P \neq P(E)$ exclusively.

From (4), the constitutive relation for the polarization amplitude $P = Ne|x|$ and the magnitude of the field squared can be written as

$$\left\{(\omega_0^2 - \omega^2 + bP^2)^2 + \frac{\gamma^2\omega^2}{m^2}\right\}P^2 = \frac{e^4 N^2}{m^2}|E|^2 \equiv S, \quad (5)$$

where $b = 3\beta/4N^2e^2m$.

The condition for the existence of bistability is the requirement that $\partial S/\partial P \rightarrow 0$, which becomes

$$(\omega^2 - \omega_0^2)/b > 0 \quad \text{and} \quad C \equiv 3\gamma^2\omega^2/m^2(\omega_0^2 - \omega^2)^2 < 1. \quad (6)$$

In this case the critical polarizations that lead to zero slope are

$$bP_c^2 = \frac{1}{3}(\omega^2 - \omega_0^2) \{2 \pm (1 - C)^{\frac{1}{2}}\}. \quad (7)$$

The minimum switch-on power occurs when the damping is very small and $C \ll 1$. In this case the critical power for switching to the higher branch is

$$bS_{\min} = 12/(\omega^2 - \omega_0^2).$$

However, since the maximum value for $\omega^2 - \omega_0^2 = m/\sqrt{3} \gamma \omega$, the minimum critical power is $S_{\min} = 12\sqrt{3} \gamma \omega / mb$.

Expression (5) for the magnitude of the flux of the electric field S as a function of the polarization is single-valued and shown in figure 4. This result can be seen to lead to a bistable

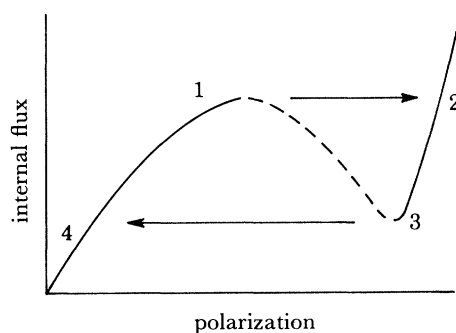


FIGURE 4. Nonlinear constitutive relation that results from the Duffing oscillator. Field squared, inside the medium, plotted as a function of the internal polarization. The field is single-valued in the polarization, but the polarization is not single-valued in the field.

polarization as a function of field, since for a given value of the field there are several values of the polarization. Bistability (or multistability) in the polarization manifests itself in a large number of observable macroscopic effects. Among these are phase bistability, which may be converted to an intensity bistability, and a bistability in both the reflected intensity and refracted angle. Further details about these macroscopic manifestations are shown in the other contribution by Garmire & Goldstone (this symposium).

The realization that expressing the electric field as a function of the macroscopic polarization may produce bistability encourages us to look in more detail at nonlinear constitutive relations from first principles. This has been done effectively in absorptive cases and for changes of state that are electric-field driven. In this paper we have shown the possibility of bistability in the polarization by using the Duffing oscillator model. Quantum mechanical formulations should also demonstrate bistability under appropriate conditions.

This work was supported by the National Science Foundation.

REFERENCES

- Dalal, V. L., Hicinbothem, W. A. Jr, Kressel, H. 1974 *Appl. Phys. Lett.* **24**, 184–5.
 Gibbs, H. M., McCall, S. L., Venkatesan, T. N. C., Gossard, A. C., Passner, A., Wiegmann, W. 1979 *Appl. Phys. Lett.* **35**, 451–453.
 Hill, J. R., Parry, G., Miller, A. 1982 *Optics Commun.* **43**, 151–153.
 Kane, E. O. 1957 *J. phys. Chem.* **1**, 249–254.

Miller, D. A. B. 1981 *J. quant. Electron.* **17**, 306–311.

Miller, D. A. B., Seaton, C. T., Prise, M. E., Smith, S. D. 1981 *Phys. Rev. Lett.* **4**, 197–199.

Miller, D. A. B., Smith, S. D., Johnston, A. 1979 *Appl. Phys. Lett.* **35**, 658–661.

Moss, T. S. 1980 *Physica Status Solidi B* **101**, 1980–1982.

Poole, C. D., Garmire, E. 1984a *Appl. Phys. Lett.* **44**, 364–366.

Poole, C. D., Garmire, E. 1984b *Optics Lett.* (Submitted.)

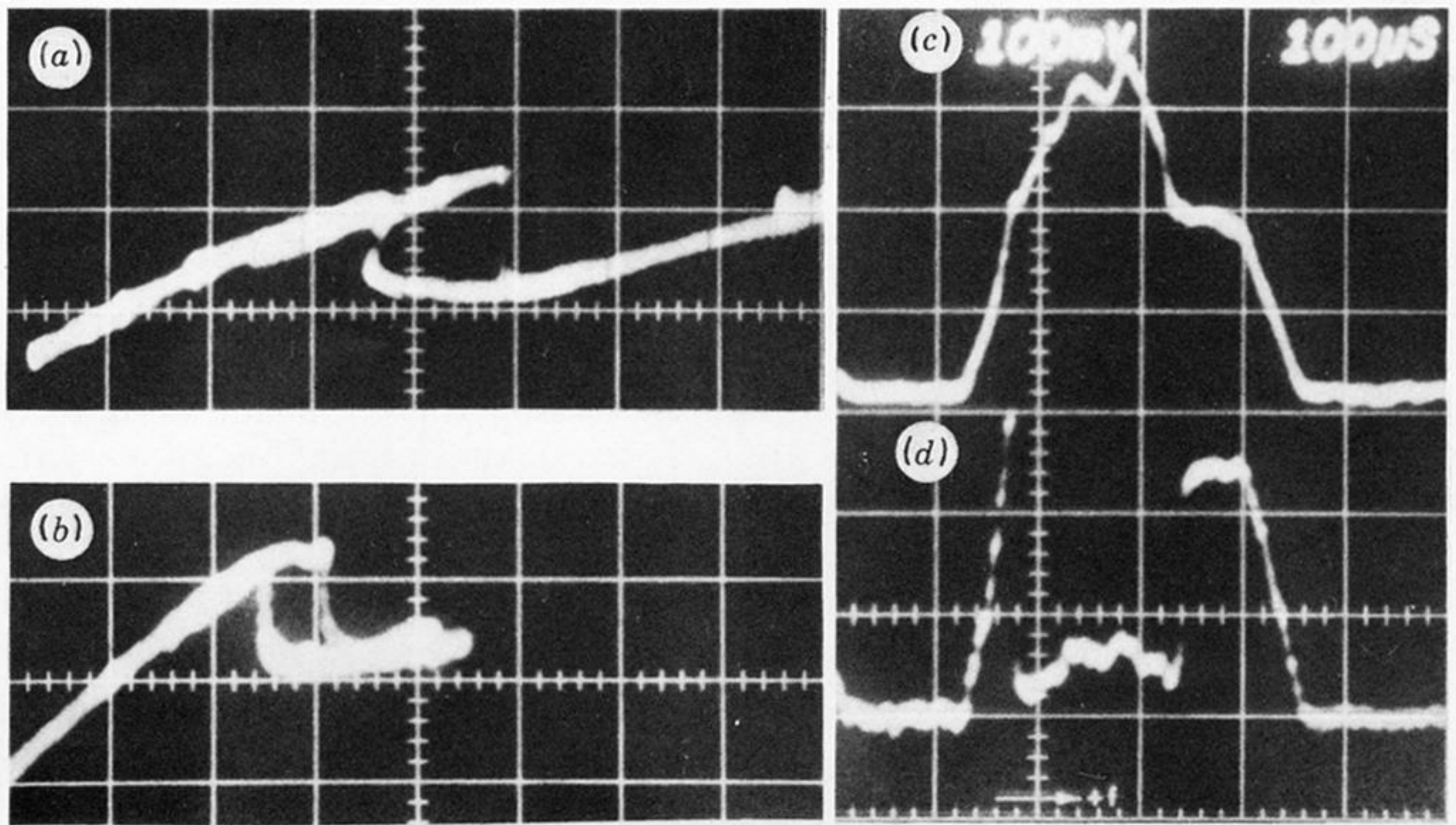


FIGURE 1. Experimental results on whole-beam bistability in InAs. (a), (b) Reflected power against incident power for two different detunings; horizontal scale is 1.5 mW per division, vertical scale is 1 mW per division. (c), (d) Input and reflected signals, respectively, as a function of time.